doi:10.2533/chimia.2010.145 Chimia 64 (2010) 145–149

Self-Assembly of Iron Oxide-Poly(ethylene glycol) Core–Shell Nanoparticles at Liquid–Liquid Interfaces

Lucio Isa§*, Esther Amstad, Marcus Textor, and Erik Reimhult

§SCS Mettler-Toledo Award Winner (Oral Presentation)

Abstract: Nanoparticles (NPs) play an increasingly important role in the fabrication of functional advanced materials. Two major steps need to be carried out in order to achieve control of the material properties. First of all, the properties of the single NPs have to be under control, especially in relation to colloidal stability; aggregation and corrosion negate all the benefits associated to the nanoscopic dimensions. Secondly, the assembly process has to be controlled to achieve a material with the desired properties. We propose here to use stabilized ceramic NPs consisting of a magnetite core, coated by a poly(ethylene glycol) (PEG) shell and study their assembly at polar/non-polar liquid interfaces, en route to fabricating functional NP membranes. These NPs show extraordinary stability in aqueous solutions achieved by anchoring linear PEG chains through an end-terminating nitroDOPA group to their surface. Furthermore, the core and shell sizes of these NPs can be independently varied with ease. We first describe the details of the NP synthesis and stabilization in bulk solutions, discussing the PEG molecular weight needed to achieve bulk stability. Subsequently, we demonstrate self-assembly of these particles at liquid–liquid interfaces (SALI) into monolayers of stable properties. SALI has been chosen as path for the assembly given its suitability for fabricating two-dimensional materials. We report here results from pendant drop tensiometry which illustrate the kinetics of NP adsorption at the liquid–liquid interface and highlight the role played by the molecular weight of the PEG shell in the interfacial assembly. In particular we show that the requisites to ensure particle stability at a liquid interface are more stringent compared to the bulk case.

Keywords: Core-shell · Iron oxide nanoparticles · Liquid–liquid interfaces · Self-assembly · Stabilization

Introduction

The last two decades have seen an upsurge in the use of inorganic nanoparticles (NPs) in many technological applications. Due to their size and extreme surface to volume ratios, NPs in the low nanometer range exhibit extraordinary properties *e.g.* in terms of magnetization, chemical activity, light absorption and scattering. They are commonly used in biosensing,[1] therapeutics[2] and as contrast agents for magnetic resonance imaging.[3]

In addition to exploiting the single nanoparticle properties, NPs are also used as 'additives' to improve the performance of existing materials[4] (*e.g.* thermal conductivity[5]), or to impart new functions to them (*e.g.* magnetic[6]). Nanoparticle composite materials often suffer from lack of microstructural uniformity (order) and NP aggregation during processing and use. Order is highly desirable to exploit coupling and collective phenomena while aggregation negates any benefit associated with the nanoscopic dimensions. A robust way to obtain nanoparticle composites is to self-assemble NPs from solution. In order to direct the self-assembly effectively one has to control the properties (size, stability, surface chemistry, *etc.*) of the single building block, the NP, for all environmental conditions during the assembly.

We focus here on iron oxide NPs, already used for many different applications due to their magnetic properties and good biocompatibility,[7] including diagnostics[8] and therapeutics such as hyperthermia.[9,10] Single-core NPs can be stabilized with a defined shell of high affinity, low molecular weight dispersants consisting of an anchor group covalently linked to a biocompatible polymer such as poly(ethylene glycol) (PEG) through a simple 'grafting to' approach.[11–15] Such dispersants adsorb on the iron oxide NP surface in a well defined way which allows for close control over the interfacial chemistry and hydrodynamic diameter. The latter is solely determined by the iron oxide core diameter and the dispersant molecular weight, packing density and solubility, all parameters which are possible to tune. We have recently demonstrated that particles of superior stability are obtained using PEG anchored with catechol derivatives.[16,17] In particular nitrocatechols such as nitroDOPA were shown to lead to irreversibly anchored dispersants at very high density, which leads to colloidal stability also at high temperature.[17]

In this article, we first briefly report on how the iron oxide NP synthesis route can be used to tailor the core size and how our novel dispersant stabilization protocol can be used to tailor independently the polymer shell thickness through simply changing the heating time of the iron oxide cores and the PEG molecular weight respectively. The effect of dispersant molecular weight on bulk NP colloidal stability is described.

Secondly, we explore the possibility of self-assembling the NP building blocks into two-dimensional films at the interface between two immiscible liquids. Self-assembly at liquid–liquid interfaces (SALI) is particularly suited to produce two-dimensional assemblies due to three key factors: i) particles are localized (trapped)

*Correspondence: Dr. L. Isa
Laboratory for Surface Science and Technology
Eidgenössische Technische Hochschule Zürich
Wolfgang-Pauli-Strasse 10, HCI G543
CH-8093 Zürich
Tel.: +41 44 633 63 76
Fax: +41 44 633 10 27
E-mail: lucio.isa@mat.ethz.ch

at the interface but ii) still maintain lateral mobility and iii) specific interactions appear at liquid–liquid interfaces, including long range dipolar repulsion and hydrodynamics-mediated attraction which can be exploited for the creation of complex structures.[18,19] Recently, SALI has been employed to create ultrathin structures such as membranes and capsules,[20–22] which could be used for drug encapsulation and delivery.[23] The most advanced example to date, demonstrated by Emrick, Russell and co-workers, made use of tri-*n*-octylphosphine oxide (TOPO)-stabilized CdSe nanoparticles at water/toluene interfaces[24] but the coordination binding of the phosphine anchor offers only low stability as well as low control over the shell thickness and homogeneity, especially if the core size is increased. Furthermore, the use of a rather rigid, thin, hydrophobic shell is likely to lead to aggregation at the oil–water interface and preclude the possibility of controlling larger particle spacings, which might instead be possible if osmotically repulsive shells are used. Thus, investigations over the effect of shell thickness on interfacial assembly for sterically stabilized particles (soluble in the aqueous phase) are still lacking and would likely lead to new insights of technological significance.

We report here measurements which demonstrate the rich and well-defined surface activity of our well-characterized core-shell NPs with complete dispersant and colloidal stability in the aqueous phase. Moreover, we discuss the influence of the dispersant molecular weight on the nanoparticle assembly, highlighting that the requirements for stability at a liquid interface may differ from the ones in bulk solutions. Finally we show experimental evidence of the formation of saturated particle layers after SALI.

Results and Discussion

Nanoparticle Synthesis and Stabilization

Iron oxide cores were synthesized by a microwave assisted non-aqueous sol–gel route.[25] The core diameter could be tuned by adjusting the heating time of the precursor dispersion. Varying the time of the precursor heating up to 30 minutes at 180 °C leads to the synthesis of nanoparticles with diameters (*d*) ranging from 5 to 15 nm, as obtained from X-ray diffraction (XRD) and analysis of transmission electron microscopy (TEM) images (Fig. 1). This core size is well below the threshold for ferromagnetic particles and thus we obtain superparamagnetic NP cores; the mono-crystalline structure of the NP cores can be seen in the high-resolution TEM image of Fig. 2. Ferromagnetic cores magnetically interact with each other even in the absence of an external magnetic field, which compromises colloidal stability and might also influence nanoparticle assembly at liquid–liquid interfaces.

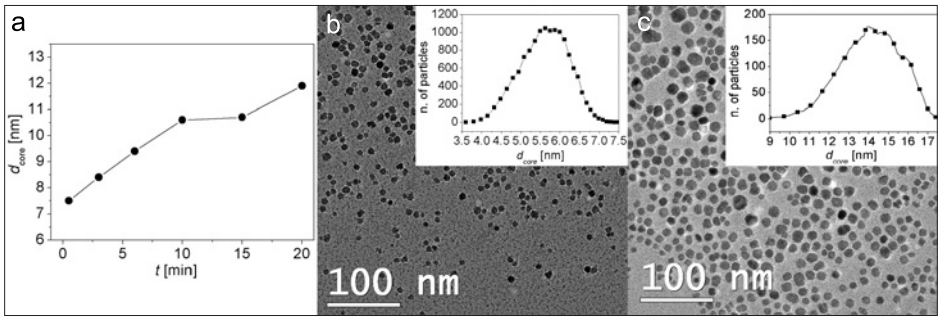

Fig. 1. a) Core size versus heating time from XRD measurements of PEG-nitroDOPA stabilized iron oxide NPs kept at 180 °C for *t* minutes. TEM micrographs for heating at 180 °C for b) 3 min and c) 30 min respectively. Insets: core size distributions from TEM images of the batches in b) (>13000 particles, d = 5.7±0.6 nm) and c) (>7000 particles, d = 14.2±1.2 nm) respectively. These particles were synthesized with a slightly different temperature ramp than those analyzed for graph a), but showed an equivalent morphology.

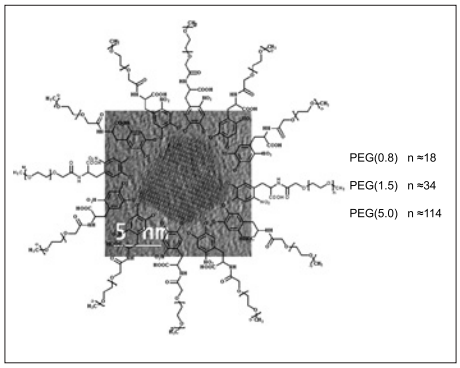

Fig. 2. Schematics of particle stabilization with PEG-nitroDOPA. The polymer formula is overlaid to a high resolution TEM micrograph of a particle in the batch in Fig. 1b). The magnetite mono-crystalline structure is evident.

In our previous work we have demonstrated that the choice of the PEG anchor group has a strong effect on NP stability both under physiological conditions and in aqueous suspensions at elevated temperatures; in particular we reported that the highest stability was obtained using nitroDOPA as anchor (Fig. 2).[17] Following this finding, we explore here the effect that changing the molecular weight of the PEG-nitroDOPA chains has on particle stability.

A first step towards a well-defined system for SALI is a system that is stable in the aqueous bulk phase. For this purpose we first determined the NP stability for the different PEG dispersants for bulk dispersions at physiological salt concentration as function of temperature. Raising the temperature and adding salt makes it possible to distinguish between weakly sterically stabilized particles, which agglomerate irreversibly as the PEG-brush loses solubility, from strongly stabilized particles, which only show low and reversible aggregation for temperatures up to 90 °C.[17] Nanoparticle stability was primarily investigated with dynamic light scattering (DLS) by analyzing scattering count rates as a function of temperature. Because the scattering intensity scales with r^6, count rates are very sensitive to nanoparticle agglomeration. Thus, an increase in count rate indicates an increase in particle size, which here corresponds to nanoparticle agglomeration, until the particle aggregates are large enough to precipitate out of solution at which point the count rate drops dramatically.

Iron oxide cores with a diameter of 5.7 nm stabilized by three PEG-nitroDOPA molecular weights: 0.8, 1.5 and 5 kDa, were investigated in this way. No significant difference in nanoparticle stability was measured between the particles stabilized with PEG of molecular weights 1.5 and 5 kDa respectively, as evidenced by only marginally and reversibly increasing count rates with increasing temperature (Fig. 3). In contrast, particles stabilized by the smaller PEG(0.8)-nitroDOPA showed the characteristic increase in count rate for aggregation followed by a rapid decrease in count rate as aggregates precipitated out of solution with increasing temperature. The larger error bars are a consequence of higher polydispersity also stemming from aggregation. Despite PEG(1.5)-nitroDOPA resulting in a thinner dispersant layer surrounding the iron oxide cores compared to PEG(5)-nitroDOPA, the former is sufficient to ensure stabilization in bulk condition even at high temperature in physiological salt concentrations. The cut-off molecular weight for bulk stability seems therefore to be *ca.* 1 kDa.

Interfacial Adsorption Results

We have discussed above the importance of choosing the right dispersant bind-

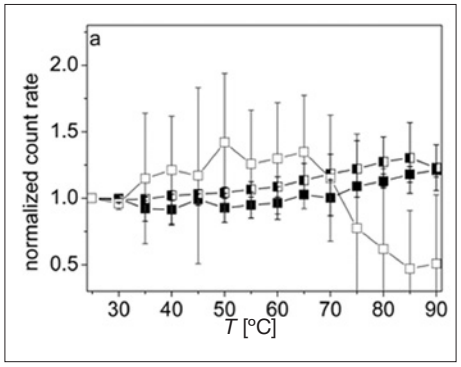

Fig. 3. Influence of PEG molecular weight on stability in solution. Temperature-dependent count rates normalized to the count rate at room temperature of d = 5.7 nm iron oxide nanoparticles stabilized with PEG(0.8)-nitroDOPA (□), PEG(1.5)-nitroDOPA (◧) and PEG(5)-nitroDOPA (■) respectively. Statistics were collected on 4–5 independent identical samples.

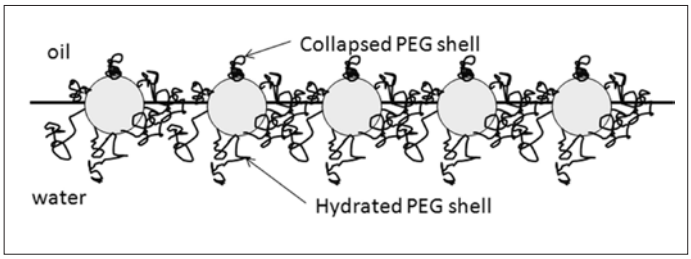

Fig. 4. Schematics of core-shell NPs at a liquid–liquid interface.

ing group and molecular weight to ensure NP stability in *bulk* solution. An *a priori* different matter is whether colloidal stability is retained at a fluid interface. While the affinity of the chosen anchor group should not be affected,[26] the different solubilities of the stabilizing polymer shell might lead to changes in steric repulsion as well as additional inter-particle interactions. The reason for particle trapping at liquid–liquid interfaces has been extensively discussed in the literature.[18] The accepted explanation by Pieranski hinges upon a free energy gain for the system related to the removal of interfacial area between the two fluids when a particle of radius r sits at the interface. The free energy gain is $\Delta F = -\pi r^2 \gamma_{ow} (1 - |\cos\theta|)^2$, where the contact angle is determined by Young's equation, $\cos\theta = (\gamma_{po} - \gamma_{pw})/\gamma_{ow}$ according to the particle-oil γ_{po}, particle-water γ_{pw} and water-oil γ_{ow} interfacial tensions.[27] The situation is more complicated if the particles have a dual, core-shell nature. The lowering of the interfacial energy by particle adsorption no longer depends only on the size and wetting properties of the core but also on the solubility of the polymer shell in the two solvents. In the case of our PEG-coated NPs, the polymer shell has a very limited solubility in the oil phase, and therefore in the energy balance we have to take into account the energy penalty coming from exposing PEG to the oil phase. Literature gives solubilities for PEG in n-decane of 0.4 and 2.2% mol for PEG(0.2) and PEG(0.4) respectively, and predicts a trend of slow increase for higher molecular weights.[28] Given these values, the portion of the stabilizing shell exposed to the oil phase will be more or less collapsed depending on molecular weight while the one remaining in water will stay hydrated (Fig. 4). The partial collapse of the polymer shell may translate into a loss of particle stability at the interface with particles agglomerating there, leading to non-uniform coverage and likely loss of NP functional properties of the resulting film. Different PEG sizes may thus lead to different stability properties at the interface. On the other hand, in the presence of stable NPs at the interface, the size of the polymer shell determines the inter-particle spacing which is a crucial parameter in the assembly of functional two-dimensional materials.

A very useful way to look at NP SALI is pendant drop tensiometry (PDT). The technique is widely used to study interfacial assembly of surfactants and proteins[29] but it has only recently been applied to nanoparticles.[24] In the static mode, a droplet of a fixed volume of the aqueous nanoparticle suspension is produced in the surrounding non-polar fluid phase (*e.g.* n-decane) and, by imaging its contour, the interfacial tension (γ) is obtained versus time. NP adsorption and structural rearrangements at the liquid-liquid interface alter γ resulting in a change of the droplet profile. It is thus possible to follow NP interfacial adsorption in real time, with high resolution and for very long periods, allowing the user to determine surface coverage and model the kinetics. Here we focus on a qualitative description of the adsorption kinetics with emphasis on the NP stability at the liquid interface.

We measured the time evolution of γ of droplets of aqueous suspensions of equal molarities of iron oxide NPs stabilized with PEG(1.5)-nitroDOPA and PEG(5)-nitroDOPA respectively, immersed in n-decane at room temperature as a function of the bulk nanoparticle concentration c (Fig. 5). PEG(0.8)-nitroDOPA was not used since particle aggregation occurred already in the bulk over the time frame of the experiments.

We measured a reduction of the interfacial tension with time both for PEG(1.5)-nitroDOPA and PEG(5)-nitroDOPA, which demonstrates that the core-shell nanoparticles are indeed surface active and adsorb at the droplet interface. However, the behaviour as a function of time changes with NP concentration and PEG molecular weight as shown by several features in Fig. 5. First of all the starting level of γ (γ_0) depends on particle concentration; during droplet formation, convection brings NPs to the interface resulting in non-zero interfacial coverage already at the beginning of the measurement. This translates into a lower γ_0 value compared to the pure water–decane case (52 mN m^{-1} at room temperature[30]) for all particles apart from the low concentration PEG(1.5)-coated ones ($c \leq 9.7 \times 10^{-3}$ mol m^{-3}), for which the values are comparable to the pure liquid system. γ_0 then decreases with increasing NP concentration.

From the respective values of γ_0, the interfacial tension decreases further as a consequence of greater amounts of NPs adsorbed at the interface, with more concentrated systems showing decay at increasingly short times. We also observe that the decay in γ shows multiple dynamical regimes. In particular, taking the example of the 9.7×10^{-3} mol m^{-3} PEG(5)-nitroDOPA particles in Fig. 5, we observe a marked slowing down of the adsorption dynamics at around 10 seconds. Furthermore, the time to reach this transition decreases with increasing NP bulk concentration but the γ level at which it happens is independent of c. The value also seems to be weakly dependent on the PEG size (~34.5±1 mN m^{-1} for both 1.5 kDa and 5 kDa). We attribute this transition to crowding effects on the interface; above a critical surface coverage[31] adsorption of additional particles is kinetically limited as they have to wait until the ones already present at the interface rearrange to leave enough space for further adsorption. The highest concentrations (9.7×10^{-2} mol m^{-3} both for PEG(1.5) and PEG (5)) are in this regime already at the beginning of the experiment.

The 9.7×10^{-3} mol m^{-3} PEG(5)-nitro DOPA curve in Fig. 5 also exhibits a second transition at around 1000 seconds. This second transition only takes place for the PEG(5) particles and only for concentrations larger than $c^* = 5.8 \times 10^{-3}$ mol m^{-3} With the second transition the final level of the interfacial tension, and therefore the NP coverage at the interface, saturates and becomes independent of the initial bulk concentration at ~28.5 mN m^{-1}. This is a strong indication of the formation of a

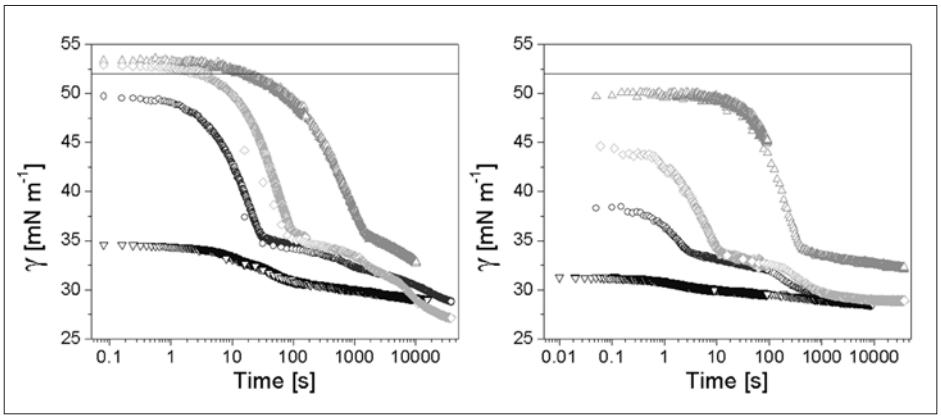

Fig. 5. Time evolution of γ of suspensions of iron oxide NPs at the water/n-decane interface from PDT. Left: PEG(1.5) coated particles; right: PEG(5) coated particles. (Δ) 1.94×10^{-3} mol m^{-3}, (→) 9.7×10^{-3} mol m^{-3}, (○) 1.94×10^{-2} mol m^{-3}, (▽) $9.7\ 10^{-2}$ mol m^{-3}. The solid line is the tabulated value of γ for a pure water in n-decane droplet.[30]

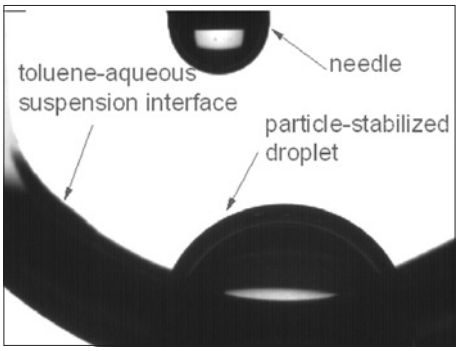

Fig. 6. Image of a droplet coated with a layer of iron oxide PEG(5)-nitroDOPA NPs ($c = 3.5 \times 10^{-1}$ mol m^{-3}) resting on a large interface between toluene and the same NP aqueous suspension. The presence of NPs on the surface of both the droplet and the large interface ensured that the two did not coalesce for minutes. In the top part of the figure, the needle used for the pendant drop measurement is visible.

saturated stable monolayer; for $c \geq c^*$ the maximum number of NPs at the interface is attained and increasing c just speeds up the formation of a complete monolayer. Furthermore we can ascribe the presence of a defined transition as stemming from a required structural rearrangement of the NPs at the interface, going from a dense disordered ensemble after the first transition, to a close-packed monolayer after saturation.

The absence of saturation in the interfacial tension for PEG(1.5) particles can be interpreted as a lack of particle stability at the interface. Despite ensuring stability in bulk, the thickness of the PEG(1.5) shell may not be sufficient to provide steric stabilization at the interface. Partial collapse of PEG in the oil phase reduces the inter-particle distance to the extent that the lower thickness of the PEG(1.5) shell fails to prevent particle aggregation by steric repulsion. Thicker shells like PEG(5) can still keep particles sufficiently apart to prevent aggregation, either by providing larger spacing with hydrated polymers in the water phase or by exhibiting a thicker collapsed shell in the part exposed to the oil. Aggregation at the interface leads to continued adsorption of NPs and the absence of reproducible formation of a close-packed, saturated monolayer of particles.

Finally we point out experimental evidence of the presence of a NP layer at the interface. Fig. 6 shows an image in which a droplet of the NP suspension is resting on a large water/toluene interface. The droplet and the lower bulk phase both have the same concentration (3.5×10^{-1} mol m^{-3}) of PEG(5)-nitroDOPA iron oxide NPs, which is well above the value for reaching a full coverage and the NPs have been left self-assembling overnight to ensure the formation of a saturated NP monolayer. As a result of the presence of the monolayers coating the two interfaces, the droplet could sit on the lower water-toluene interface for minutes without coalescing, indicating that the formed monolayer is stable to additional adsorption and aggregation even when in direct contact with a second particle film.

Conclusions

We have demonstrated the synthesis and the stabilization of core-shell iron oxide NPs using microwave synthesis and a novel anchor chemistry with which we can easily and independently tune the size of the cores and of the stabilizing polymer shell. In particular, it was shown that despite the high grafting density and anchor stability, PEG(0.8)-nitroDOPA does not create a sterically stabilizing shell of sufficient thickness to prevent aggregation under physiologic conditions, while for PEG-nitroDOPA molecular weights ≥1.5 kDa perfect stabilization under physiological salt concentrations and at high temperature was achieved. The presence of a minimum shell thickness for bulk solution stability has also been recently reported in the literature for phosphate-PEG[32] and PEG-silanes.[33] Furthermore, we have demonstrated that such core-shell NPs can be used as building blocks for two-dimensional assemblies at the interface between two liquids by investigating their interfacial adsorption using PDT. From observing the long time behaviour at concentrations above a critical value we have deduced that the requirements for steric stabilization are more stringent at the oil–water interface than in the aqueous bulk. Higher molecular weight (thicker) PEG shells are needed to prevent aggregation at the interface and in particular PEG(1.5) is no longer sufficient to provide an effective steric barrier, as opposed to PEG(5). We have demonstrated that PEG(5)-nitroDOPA NPs can indeed be used for SALI and lead to the formation of a saturated NP monolayer above a critical bulk concentration. Concluding we believe that core-shell nanoparticles constitute an extremely promising system not only to assemble composite materials but also to investigate interfacial adsorption of more complex objects. The extraordinary, independent control over both the core and shell properties, once the dispersant binding has been optimized, allows fabrication through SALI of ultra-thin functional materials of linked NP cores at defined separations tailored by the polymer shell. For instance, we envisage the use of elastic polymers that are terminated by cross-linkable groups so that, after SALI, the NP ensemble can be made into a detachable, mechanically stable membrane to be applied in numerous high-end situations including *e.g.* lab-on-chip applications and miniature actuators.

Experimental

Iron Oxide Nanoparticles

Iron oxide nanoparticles were synthesized according to Bilecka *et al.*[25] Briefly, 173 mg $Fe(ac)_2$ (Sigma-Aldrich, batch 517933, Lot 03901JJ) was dissolved in 5 ml benzylalcohol (Acros). Using a power of 300 W, the solution was heated to 180 °C in a microwave (Discover S-class, CEM, NC, USA). This solution was kept at 180 °C for different times before it was cooled to 60 °C with a N_2 stream. The resulting nanoparticles were washed once with 10 ml ethanol (Scharlau) before they were re-dispersed in 10 ml ethanol resulting in an iron oxide nanoparticle concentration of approximately 10 mg/ml. Washed iron oxide nanoparticles were kept at 4 °C for 2–6 h. PEG-nitroDOPA synthesized

as described in ref. [7] was aliquoted in N,N-dimethylformamide (DMF) (Sigma-Aldrich) at a concentration of 100 mg/ml. 6 mg of PEG-nitroDOPA was added to 1 ml of EtOH followed by the addition of 1 mg of iron oxide nanoparticles. This suspension was kept at 50 °C for 24 h under constant mechanical stirring at 500 rpm (Thermomixer comfort, Vaudaux-Eppendorf, Switzerland). Excessive dispersants were removed by 24 h dialysis against Millipore water (R = 18.2 Ω, TAC<6 ppb) using dialysis membranes with a cut-off of 24 kDa (Spectra/Por dialysis membrane, spectrum labs, Netherlands) before so-stabilized iron oxide nanoparticles were freeze-dried (freeze dryer ALPHA 1-2 / LDplus, Kuhner LabEquip, Switzerland) and re-dispersed in Millipore water at a concentration of 10 mg/ml.

Nanoparticle Characterization

Dynamic light scattering (DLS) experiments were run on a Zetasizer Nano ZS (Malvern, UK) in the 173° backscattering mode as described in ref. [17]. Briefly, temperature-dependent DLS experiments were performed in 4-(2-hydroxyethyl)-1-piperazineethanesulfonic acid (HEPES) (Sigma-Aldrich) containing 150 mM NaCl at an iron oxide nanoparticle concentration of 200 µg/ml. Solutions were filtered with 200 nm Minisart syringe filters (Sartorius, Germany) prior to DLS analysis to eliminate dust. These suspensions were heated from 25 to 90 °C in 5 °C steps with 10 min equilibration time before the respective DLS experiment.

X-ray diffraction was performed in the reflection mode on a Philips PW1800 instrument equipped with a post-sample monochromator. Spectra were acquired using a Co K_α source. The nanoparticle size was calculated with the Scherrer formula based a Gaussian fit of the (311) peak.

Transmission electron microscopy was performed on a Philips CM12 microscope operated at 100 kV. Iron oxide nanoparticles suspended in Millipore water at a concentration of 1 mg/ml. A 3.5 µl droplet was dried on a 10 nm carbon coated 400 mesh Cu-grid. TEM images were analyzed to obtain the iron oxide core size. The image analysis was performed with a custom written IDL code (ITT Visual Information Solutions) based on the Crocker and Grier algorithm.[34] Briefly, images were filtered with a spatial band-pass filter to eliminate long range contrast variations and high frequency instrumental noise. After filtering, the intensity-weighted centre of mass of each feature was found and the respective diameter calculated.

Pendant Drop Tensiometry (PDT)

PDT experiments were performed with a drop shape analysis system (DSA100, Krüss, Germany). At the tip of a stainless steel needle (diameter 1.8 mm), immersed in the oil phase (*e.g.* n-decane ≥ 99%, Sigma-Aldrich), droplets of 30 µl of the aqueous NP suspension (Millipore water, R = 18.2 Ω, TAC<6 ppb) are produced at a rate of 200 µl/min at room temperature and imaged with a CCD camera as a function of time. The droplet profile is detected automatically with an analysis software (DSA3, Krüss) and fitted with the Laplace-Young equation to obtain the interfacial tension (γ) as a function of time. Experiments were normally split up into two parts: an initial part during which images were taken at a high frame rate (12.5 Hz) and a second one where the images were taken for long times at lower rates (0.25 Hz). In this way we were able to capture the fast dynamics in the initial stages of adsorption and then follow the long time evolution of γ.

Acknowledgements

The authors thank Prof. Nicholas D. Spencer and Eva Beuer for the access and use of the drop shape analysis system. We also thank Torben Gillich for the synthesis of nitroDOPA and Prof. Markus Niederberger and Idalia Bilecka for their help with the iron oxide nanoparticle synthesis. The Electron Microscopy Center ETH Zürich (EMEZ) is acknowledged for support on the electron microscopy. COST Action No. D43 'Multifunctional Superparamagnetic Iron Oxide Nanoparticles for Targeted Magnetic Resonance Imaging', Swiss National Science Foundation NCCR Project 'Nanoscale Science' and ETH Zurich are acknowledged for their financial support.

Received: January 27, 2010

[1] W. Zhao, M. A. Brook, Y. F. Li, *ChemBioChem* **2008**, *9*, 2363.
[2] S. Lal, S. E. Clare, N. J. Halas, *Acc. Chem. Res.* **2008**, *41*, 1842.
[3] C. Sun, J. S. Lee, M. Q. Zhang, *Adv. Drug Delivery Rev.* **2008**, *60*, 1252.
[4] A. C. Balazs, T. Emrick, T. P. Russell, *Science* **2006**, *314*, 1107.
[5] H. Q. Xie, J. C. Wang, T. G. Xi, Y. Liu, F. Ai, Q. R. Wu, *J. Appl. Phys.* **2002**, *91*, 4568.
[6] G. Filipcsei, I. Csetneki, A. Szilagyi, M. Zrínyi, in 'Oligomers Polymer Composites Molecular Imprinting', Springer: Berlin/Heidelberg, **2007**, Vol. 206, p. 137–189.
[7] R. Weissleder, D. D. Stark, B. L. Engelstad, B. R. Bacon, C. C. Compton, D. L. White, P. Jacobs, J. Lewis, *Am. J. Roentgenology* **1989**, *152*, 167.
[8] J. H. Lee, Y. M. Huh, Y. Jun, J. Seo, J. Jang, H. T. Song, S. Kim, E. J. Cho, H. G. Yoon, J. S. Suh, J. Cheon, *Nature Medicine* **2007**, *13*, 95.
[9] M. Namdeo, S. Saxena, R. Tankhiwale, M. Bajpai, Y. M. Mohan, S. K. Bajpai, *J. Nanosci. Nanotechnol.* **2008**, *8*, 3247.
[10] M. J. Pittet, F. K. Swirski, F. Reynolds, L. Josephson, R. Weissleder, *Nature Protocols* **2006**, *1*, 73.
[11] E. Amstad, S. Zurcher, A. Mashaghi, J. Y. Wong, M. Textor, E. Reimhult, *Small* **2009**, *5*, 1334.
[12] C. J. Xu, K. M. Xu, H. W. Gu, R. K. Zheng, H. Liu, X. X. Zhang, Z. H. Guo, B. Xu, *J. Am. Chem. Soc.* **2004**, *126*, 9938.
[13] J. Xie, C. Xu, N. Kohler, Y. Hou, S. Sun, *Adv. Mater*. **2007**, *19*, 3163.
[14] H. W. Gu, Z. M. Yang, J. H. Gao, C. K. Chang, B. Xu, *J. Am. Chem. Soc*. **2005**, *127*, 34.
[15] J. H. Gao, G. L. Liang, J. S. Cheung, Y. Pan, Y. Kuang, F. Zhao, B. Zhang, X. X. Zhang, E. X. Wu, B. Xu, *J. Am. Chem. Soc.* **2008**, *130*, 11828.
[16] E. Amstad, S. Zurcher, A. Mashaghi, J. Y. Wong, M. Textor, E. Reimhult, *Small* **2009**, *5*, 1334.
[17] E. Amstad, T. Gillich, I. Bilecka, M. Textor, E. Reimhult, *Nano Lett.* **2009**, *9*, 4042.
[18] 'Colloidal particles at liquid interfaces', Eds. B. S. Binks, T. S. Horozov, Cambridge University Press: Cambridge, **2006**.
[19] F. Bresme, M. Oettel, *J. Phys. Condens. Matter* **2007**, *17*, 413101.
[20] A. Boker, J. He, T. Emrick, T. P. Russell, *Soft Matter* **2007**, *3*, 1231.
[21] Y. Lin, H. Skaff, A. Boker, A. D. Dinsmore, T. Emrick, T. P. Russell, *J. Am. Chem. Soc*. **2003**, *125*, 12690.
[22] H. Skaff, Y. Lin, R. Tangirala, K. Breitenkamp, A. Boker, T. P. Russell, T. Emrick, *Adv. Mater.* **2005**, *17*, 2082.
[23] H. W. Duan, D. Y. Wang, N. S. Sobal, M. Giersig, D. G. Kurth, H. Mohwald, *Nano Lett.* **2005**, *5*, 949.
[24] S. Kutuzov, J. He, R. Tangirala, T. Emrick, T. P. Russell, A. Boker, *Phys. Chem. Chem. Phys.* **2007**, *9*, 6351.
[25] I. Bilecka, I. Djerdj, M. Niederberger, *Chem. Commun.* **2008**, 886.
[26] E. Amstad, V. V. Nagaiyanallur, H. Fischer, A. U. Gehring, M. Textor, E. Reimhult, in preparation.
[27] P. Pieranski, *Phys. Rev. Lett.* **1980**, *45*, 569.
[28] G. L. Gaines, *J. Colloid Interface Sci.* **1978**, *63*, 394.
[29] Q. He, Y. Zhang, G. Lu, R. Miller, H. Mohwald, J. B. Li, *Adv. Colloid Interface Sci.* **2008**, *140*, 67.
[30] S. Zeppieri, J. Rodriguez, A. L. L. de Ramos, *J. Chem. Eng. Data* **2001**, *46*, 1086.
[31] Quantified by TEM in a previous study with hard sphere CdSe NP adsorbing from the non-polar toluene phase as ~40% [24].
[32] U. I. Tromsdorf, O. T. Bruns, S. C. Salmen, U. Beisiegel, H. Weller, *Nano Lett.* **2009**, *9*, 4434.
[33] C. Barrera, A. P. Herrera, C. Rinaldi, *J. Colloid Interface Sci.* **2009**, *329*, 107.
[34] J. C. Crocker, D. G. Grier, *J. Colloid Interface Sci.* **1996**, *179*, 298.